

TOWARDS HIGH BUILD RATES: COMBINING DIFFERENT LAYER THICKNESSES WITHIN ONE PART IN SELECTIVE LASER MELTING

Michael Kniepkamp¹, Jana Harbig¹, Christoph Seyfert², Eberhard Abele¹

¹ Institute of Production Management, Technology, and Machine Tools (PTW),
Technische Universität Darmstadt, Darmstadt, Germany

² EOS GmbH Electro Optical Systems, Krailling / Munich, Germany

Abstract

Additive manufacturing of metallic parts using powder bed based fusion processes like selective laser melting is increasingly used in industrial applications. With typical layer thicknesses of 20 – 40 μm good surface qualities and high geometrical accuracy can be achieved compared to other AM processes. However, low layer thicknesses are to the detriment of build rates as more layers are required. Increasing the layer thickness can significantly increase build rates at the cost of surface quality and accuracy. In this paper a new parameter set for a layer thickness of 60 μm is developed and combinations of different layer thicknesses within one part are investigated. Thus increased build rates can be achieved while a high accuracy can be maintained when locally required. Specimens with combination of different layer thicknesses in various build orientations are produced and mechanically tested. Micrographs of the layer transitions are examined and recommendations for their design are given.

1. Introduction

Additive manufacturing (AM) is an emerging field in manufacturing technologies that has the common principle of building up solid parts directly from 3D CAD data by adding material layer by layer. Powder bed fusion based additive manufacturing processes use thermal energy to selectively fuse regions of a powder bed [1]. This study focuses on laser beam melting of metal powders, often termed Selective Laser Melting (SLM) or Direct Metal Laser Sintering (DMLS). The build time of the SLM process consists of two parts: the main time and the idle time. During the main time the laser is actively melting powder to generate a dense structure. During the idle time the machine is preparing a new layer of material. The idle time directly correlates with the layer thickness as less layers are required with a higher thickness to build a part. The main time depends on several factors and can be approximated by the product of scanning speed, hatch distance and layer thickness which represents the build rate. Previous studies showed that the process efficiency is increased with higher layer thickness as less energy is lost by reflection and conduction [2]. As a result increasing the layer thickness has a high impact on the build rates as the main and idle times are decreased. The SLM process typically involves layer thicknesses between 20 and 100 μm [3, 4] depending on the material and the spot size of the laser beam. Recent studies have shown that dense parts can also be produced with layer thicknesses up to 200 μm using high power lasers with larger spot sizes [5, 6]. The downside of increased layer thickness is the reduced surface quality [7, 8]. Surface roughness is critical for many applications. The fatigue performance of additive manufactured parts is dominated by their surface roughness [9, 10]. Typical AM parts like medical instruments and casting molds require low surface roughness for cleanability and high part qualities. To meet those demands SLM parts require post-processing operations such as

grinding, shot peening or machining. When post-processing is required anyways it is cheaper to increase the build rates by increasing the layer thickness as surface roughness is not a disadvantage anymore. A major problem of post-processing is that internal structures like channels cannot be reached. Therefore high surface qualities must be achieved during the build process. By combining low and high layer thicknesses within one part locally high surfaces qualities can be realized while maintaining high build rates.

In this study layer thickness of 20 and 60 μm are combined within one part using one laser source similar to the skin-core strategy presented by Schleifenbaum et al. [11] with a focus on the mechanical properties of both parameter sets and their intersection area. Using the given 20 μm parameter set as a reference the aim is to increase the build rate without reducing its tensile strength, yield strength or ductility. As no 60 μm parameter set was present for the used SLM system and powder combination a new parameter set is developed.

2. Research methodology

A commercial available additive manufacturing system M290 (EOS GmbH, Germany) is used for this study. This system combines a 400 W Yb - fiber laser with a spot size of 84 μm and operates in an inert gas atmosphere using Argon [12]. The building volume has a size of 250 mm x 250 mm x 325 mm. Gas atomized stainless steel 316L powder was used for all experiments in this study. An SEM analysis of the powder was used to determine the particle distribution. Particles ranging from 11 μm to 54 μm and a d_{50} of 25 μm was determined. A parameter set with a layer thickness of 20 μm qualified by the system manufacturer is used as a reference. The reference set is using the manufacturers parameter set “316L_Surface_M291 1.10” with a volume energy of approximately 100 J/mm³. The measurement of the density was done in relation to the suggested approach of Spierings and Levy [13] by using the Archimedes method. Cubes with an edge length of 10 mm were build and their density was calculated using Eq. (1).

$$\rho_P = \frac{m_a}{m_a - m_{fl}} \rho_{fl} \quad (\text{Eq. 1})$$

The total mass (m_a) in air of the cleaned, dried, and outgassed cubes was measured using a calibrated Kern ABT 220-4M scale. After measuring all the specimens in dry condition, the wet mass (m_{fl}) was balanced in a 5% tenside solution using the density of the solution (ρ_{fl}) at the given temperature. To determine the mechanical properties tensile testing was conducted using a Zwick Z100 (Zwick GmbH & Co. KG, Germany) tensile testing system with a maximum force of 100 kN. Elongation was measured using an optical videoXtens system with a resolution of 0.5 μm . Round tensile specimens type A [14] with a diameter of 5 mm and a gage length of 25 mm were used. The tensile specimens were milled out of cylinders with a diameter of 10 mm and a height of 80 mm to prevent an influence of the surface roughness on the results. All specimen were tested in an as build condition without any additional heat treatment.

The aim of this study is to increase build rate using a multi-layer thickness approach without compromising the materials strength. The well tested reference parameter set of the system manufacturer is used as a base for the mechanical properties. Its mechanical properties were determined in a first step by measuring the density of 25 10 mm cubes equally distributed in the build space, tensile testing of 10 specimens built in a vertical orientation parallel to the built direction and 10 specimens built with an inclination of 45° to the built direction. The results are

summarized in table 1 and are well within the range of the system manufacturers given values [15] for this combination of machine, parameter set and powder.

Table 1: Mechanical properties of the reference parameter set

	Density [g/cm ³]	UTS 0* [MPa]	UTS 45 [MPa]	Rp0.2 0** [MPa]	Rp0.2 45 [MPa]	A 0*** [%]	A 45 [%]
Mean	7.9889	584.59	643.49	423.46	600.6	41.46	42.5
Std. dev	0.0023	0.92	1.4	9.56	11.82	0.94	0.57

* ultimate tensile strength, ** yield strength at 0.2%, *** elongation at break point

3. Development of a 60 μm Parameter Set

In preliminary tests, a layer thickness of 60 μm proved to be optimal for the given laser power and focus diameter to increase the build rate of the system. A layer thickness of more than 60 μm leads to an unstable process with significantly increased amount of splatter particles and flue gas. To reduce residual stress and anisotropy a rotating stripes scan strategy with a stripe width of 5 mm and a rotation angle of 67° in each layer is used for the developed parameter set. To achieve parts with a high density the right amount of energy is required to melt the powder without voids. This energy can be described with the volume energy (E_V) (Eq. 2) with the laser power (P_L), the scan velocity (v_s), the hatch distance (h_s) and the layer thickness (d). Since the layer thickness is fixed to 60 μm suitable parameters for laser power, scan speed and hatch distance have to be determined.

$$E_V = \frac{P_L}{v_s h_s d} \quad (\text{Eq. 2})$$

The energy required to melt a single scan track is described by the quotient of laser power and scan speed which is called line energy (E_L). The width of a single scan track and therefore the required hatch distance depends on the line energy, the focus diameter and the layer thickness. Considering these factors a hatch distance of 0.12 mm has been chosen as a starting point. Cubes with an edge length of 10 mm were built using different combinations of line energy and laser power. All parameter combinations are summarized in table 2.

Table 2: Parameter range to generate a process window

Parameter	d [mm]	h_s [mm]	E_L [J/mm]	P [W]
Variation	0.06	0.12	0.2 – 0.7	170 – 370

Each parameter combination was built three times and the density of the cubes was measured. The results are shown in figure 1. Within the selected parameter space it is possible to build parts with a density from 95.74 up to 99.84 % of the reference density. The highest density is present at a laser power of 220 to 270 W with line energies from 0.3 to 0.4 J/mm². To find the optimal parameter combination a parameter space around the center point (P_L 270 W, v_s 675 mm/s and h_s 0.12 mm) was investigated using a multivariate approach. The laser power was adjusted between 220 and 320 W, the scan speed between 450 and 900 mm/s and the hatch distance between 0.08 and 0.16 mm (Figure 1).

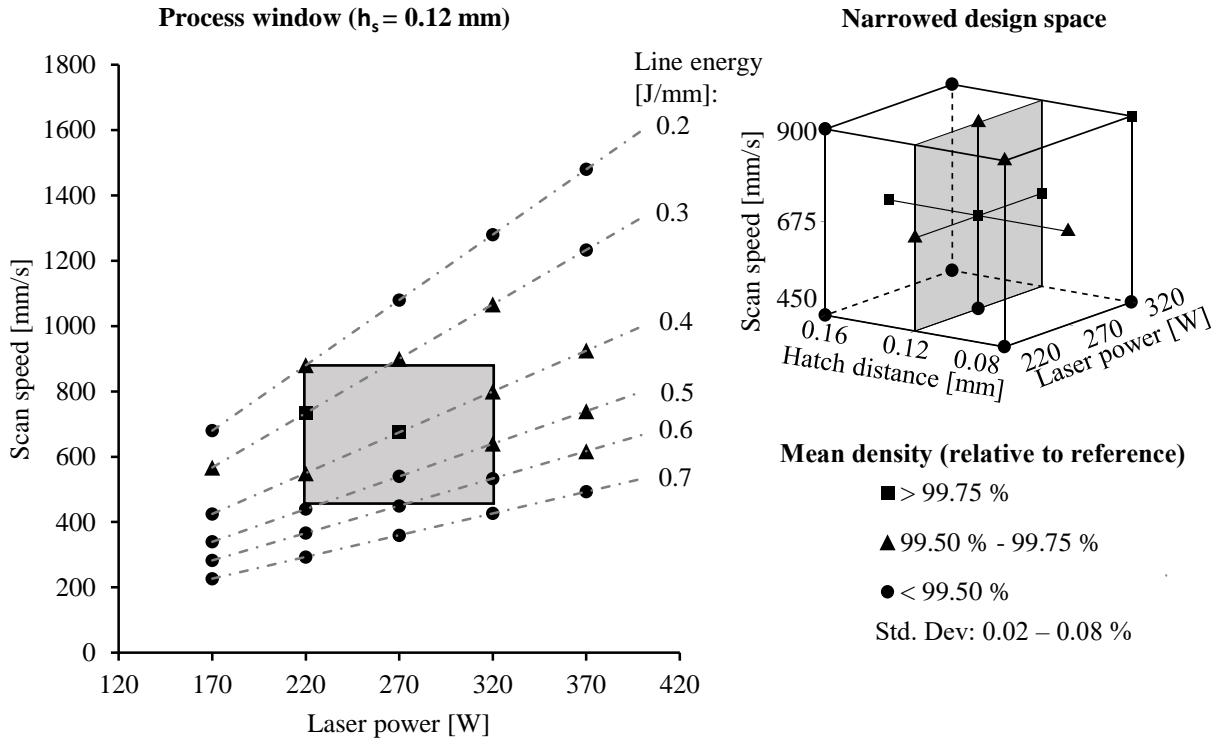


Figure 1: Process window for a layer thickness of 60 μm

Three 10 mm cubes were built with each parameter combination and the density was measured. Parts with a high relative density without internal voids or cracks are required to build parts with good mechanical properties. Tensile testing was performed for all parameter combinations which exceeded a density of more than 99.75 % of the reference parameter set. For each combination 5 specimens were built in a vertical orientation parallel to the build direction. The results of the tensile test are summarized in table 3. All selected parameter sets have an elongation of more than 40 % an ultimate tensile strength of 582 to 624 MPa and a yield strength of 492 to 522 MPa. The mechanical properties of parameter set #1 are closest to the reference parameter set but has a build rate of only 4.86 mm³/s. Parameter set 3 has the highest built rate and good mechanical properties as well. As a result parameter set 3 is selected for further testing in chapter 4.

Table 3: Tensile testing results of selected 60 μm parameter sets

#	P _L [W]	v _s [mm/s]	h _s [mm]	Density [g/cm ³]	Rel. Dens. [%]	Std. Dev	Build Rate [mm ³ /s]	UTS [MPa]	Std. Dev	Rp 0.2 [MPa]	Std. Dev	A [%]	Std. Dev
1	320	675	0.12	7.9716	99.78	0.064	4.86	582.90	2.59	491.98	6.08	42.36	0.41
2	220	733	0.12	7.9764	99.84	0.018	5.28	613.65	3.49	511.72	4.02	43.02	1.33
3	270	675	0.16	7.9733	99.80	0.032	6.48	624.23	2.30	522.54	3.28	40.66	1.79
4	270	900	0.10	7.9753	99.83	0.012	5.40	602.39	1.88	502.88	14.22	43.21	1.46
5	270	675	0.12	7.9703	99.77	0.072	4.86	602.70	2.19	510.89	8.69	41.70	0.36
6	220	730	0.10	7.9738	99.81	0.079	4.38	593.70	1.74	505.19	7.70	44.71	0.74

4. Combining two layer thicknesses in one part

For industrial parts it is required to combine segments with different layer thickness in various orientations. In this study the vertical (parallel to build direction (z)), the horizontal (perpendicular to the build direction) and an orientation with an inclination of 45° is investigated as these combinations cover all the basic cases. The transition area between to segments is of particular interest since unsuitable parameters for the transition layer thickness are being used and overlapping with areas of double exposure occurs. All cases for tensile testing are shown in figure 2. In case 1 and 2 a segment with a layer thickness of $60\ \mu\text{m}$ is built on-top of a $20\ \mu\text{m}$ segment. Tensile test specimens use to break in the middle of the gage area. To determine if the transition area is causing the specimen to fail it is moved to the upper and lower third of the gauge area. Case 3 and 4 are representing a segment of $20\ \mu\text{m}$ build on top of a $60\ \mu\text{m}$ segment. Use case 5 represents the vertical combination of two segments. The melt pool in the SLM process is deeper than the layer thickness and thus the previous layer is re-melted to connect both layers without any voids. In case 5 an overlap region is required to ensure solid connection between both segments. A width of $120\ \mu\text{m}$ is selected which corresponds to the stripe overlap of the scan strategy. Cases 6 and 7 are a mix of the others with an inclination of 45° . In this case the two segments have to be securely connected in the x-y and z direction. No overlap between the two segments was selected.

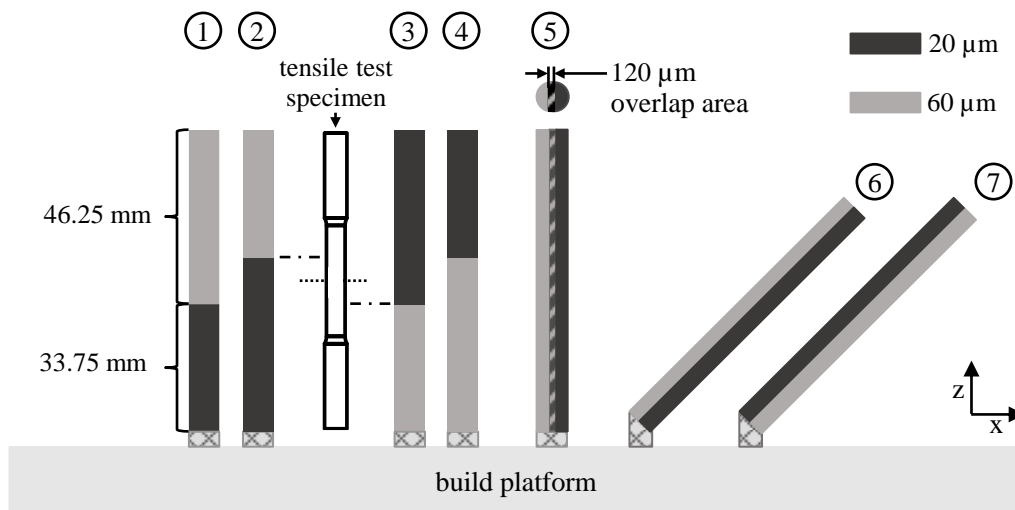


Figure 2: Tensile test specimens with different combinations of layer thickness

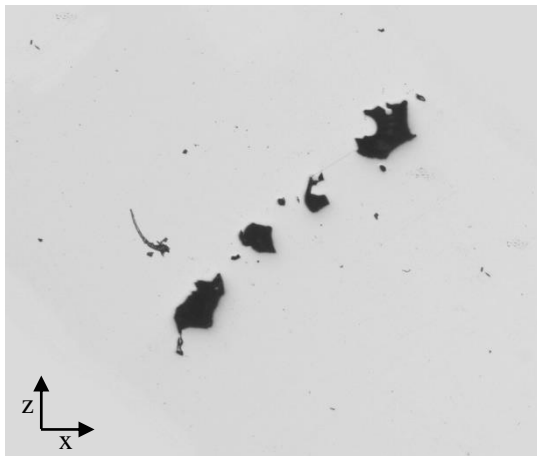
The results of the tensile tests are summarized in table 4. No specimen failed in the transition area. All specimens with horizontal aligned sections broke in the $20\ \mu\text{m}$ part of the gage area with a similar ultimate tensile strength and an increased yield strength compared to the $20\ \mu\text{m}$ parameter set. The elongation at break is significantly reduced in case 1 and 4 and is similar to the reference set in case 2 and 3. The inclined specimens of case 6 and 7 have a higher tensile strength and yield strength than the vertical ones but have a reduced elongation at break. Especially case 7 shows an elongation which is 6.85 % lower than the reference at an inclination of 45° .

Table 4: Tensile test results of hybrid specimens

#	Break Point	Mean UTS [MPa]	Std. dev.	Mean Rp 0.2 [MPa]	Std. dev.	Mean A [%]	Std. dev.
1/4	20 μm section	579.18	5.09	529.10	23.59	29.86	0.90
2/3	20 μm section	568.28	0.79	519.76	14.87	41.89	1.20
5	gauge center	594.62	2.91	530.76	26.08	39.45	3.56
6	gauge center	648.43	0.66	583.20	10.57	38.85	2.37
7	gauge center	639.80	5.67	580.44	14.53	35.65	1.84

To further investigate the transition areas micrographs have been prepared and were examined in two steps. First optical microscopy was used to detect voids and defects in polished micrographs. In the second step the polished samples were etched to make the microstructure visible using V2A-lye (100 ml distilled water, 100 ml Hydrochloric Acid, 10 ml Nitric Acid, 0.6 ml Vogel's Sparbeize) [16]. Smaller defects with a size off less than 10 μm can be seen on all polished specimens. No noticeable defects can be seen in the interface areas except for case 7. Large voids with an average equivalent diameter of 69.77 μm are present in the interface area (figure 3).

Polished Sample Case 7



Polished and Etched Sample Case 7

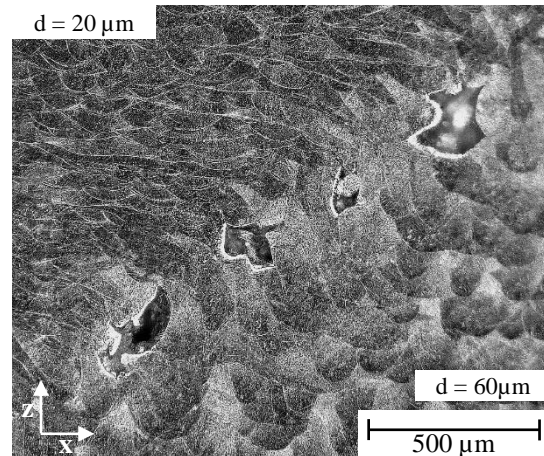
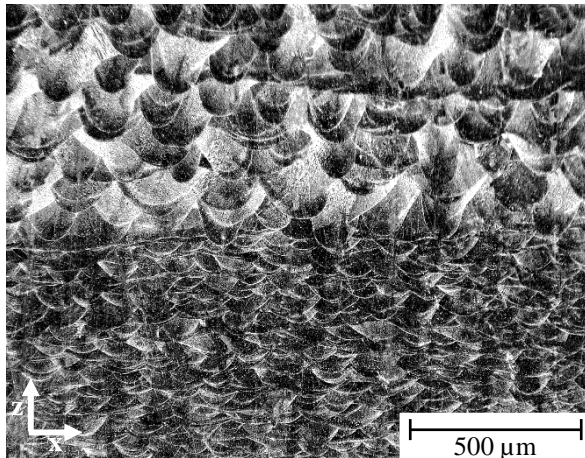


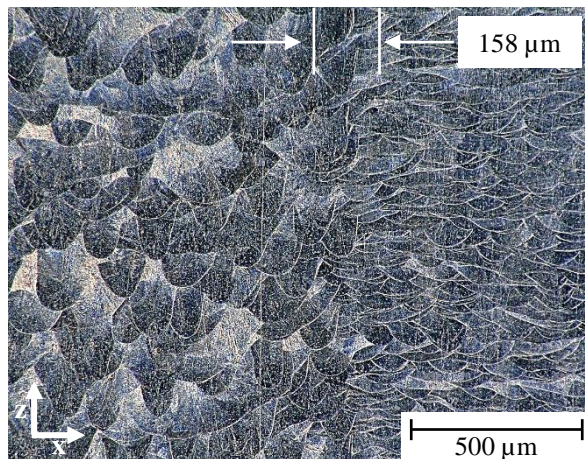
Figure 3: Micrographs of hybrid case 7

The microstructure of the interface are can be seen in the etched micrographs (figure 4). The structure of the different layer thicknesses with smaller and larger melt pools is clearly visible. In case 1 and 2 the transition from 20 to 60 μm is completed within one layer. In case 3 and 4 the two layers above the last 60 μm layer show larger melt pools than in the other 20 μm regions. In case 5 a transition area with a width of roughly 158 μm with mixed melt pool sizes from the 20 and 60 μm region is present.

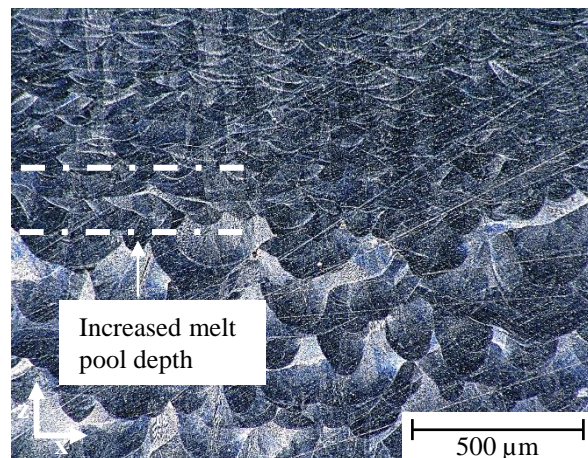
Etched micrograph Case 1 and 2



Case 5



Case 3 and 4



Case 6

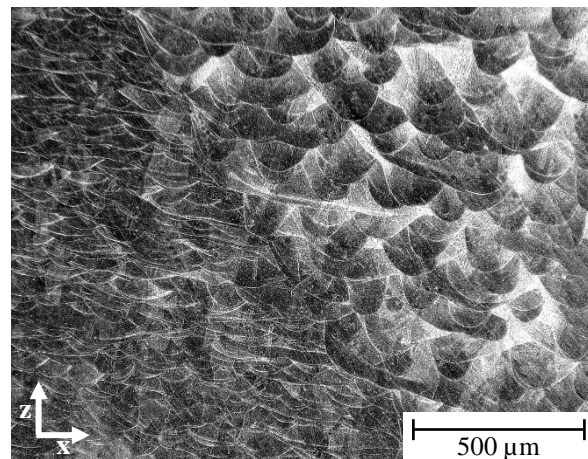


Figure 4: etched micrographs from case 1 to 6

5. Discussion

With a hatch distance of $0.12 \mu\text{m}$ a large range of scan speed and laser power can be used make parts with a density of more than 99.5 % using a layer thickness of $60 \mu\text{m}$. With process costs in mind high laser powers and scan speeds can be used to achieve build rates of up to $10 \text{ mm}^3/\text{s}$ with a density of more than 99 %. Without reducing the mechanical properties the optimal parameter window is present at lower build rates from 4.86 to $6.48 \text{ mm}^3/\text{s}$. The decrease in density at higher laser powers and scan speeds can be explained with the increased cooling rates at higher speeds coupled with disadvantageous melt pool dynamics. To further increase build rates a larger focus diameter is required to utilize higher laser powers at lower scan speeds [17]. With a layer thickness of $20 \mu\text{m}$ a volume energy of $100 \text{ J}/\text{mm}^3$ is required to achieve the highest density. Using a layer thickness of $60 \mu\text{m}$ similar densities can be achieved with only $42 \text{ J}/\text{mm}^3$. This increase of process efficiency has also been reported by Meiners [2] and can be explained with the decrease of the conductive heat loss into the previous built layers. The ultimate tensile strength and the yield strength of the selected $60 \mu\text{m}$ parameter set are increased by 6 % compared to the reference set. This difference has a great impact on the fracture behavior of the hybrid specimens. The slightly

decreased ductility of the 60 μm parameter set is inducing an early plastic deformation in the 20 μm section. This is further increasing the stress in the 20 μm section which results in a break in the 20 μm section in all horizontal hybrid specimens. The overall elongation of the specimen is significantly decreased in case 1 and 4 as the 20 μm section is only 1/3 of the gage area and the 60 μm is not contributing to the elongation as no or very low plastic deformation is present. Since none of the horizontal specimen broke in the interface are no special process strategy is required in those use cases. The inclined specimens of case 7 have a significantly reduced ductility compared to the reference set and the 60 μm set. This is caused by large pores in the interface area which locally increase stress and cause an early break of the specimen. The microstructure of the transition area can be explained with the actual powder layer thicknesses. The bulk density of powders (ρ_b) used in selective laser melting ranges from 50 to 60 % ($\rho_b = 0.5 - 0.6$). Assuming the first applied layer has the desired thickness of (d) the actual applied powder layer thickness (d_p) before melting can be calculated using equation 3.

$$d_{p(n=1)} = d; d_{p(n=2)} = d + d_{p(n=1)}\rho_b; d_{p(n=3)} = d + d_{p(n=2)}\rho_b; \dots \quad (\text{Eq. 3})$$

Several methods exist to determine the bulk densities of metal powders but measuring the actual bulk density for the given combination of powder, coater blade geometry and rake mechanism is a challenging task. Calculating the powder layer thickness with a bulk density of 50 % ($\rho_b = 0.5$) using equation 2 results in a powder layer thickness of

$$d_p = \frac{d}{1 - \rho_b} \quad (n = \infty) \quad (\text{Eq. 4})$$

Changing the layer thickness within on part results in a transition from one powder layer thickness to another. The calculated powder layer thickness from 20 μm to 60 μm and from 60 μm to 20 μm is shown in figure 5. The volume energy for a parameter set in the SLM process is optimized for a constant powder layer thickness (Section 2). In the transition area 4 layers are required to adjust the powder layer thickness to the new layer thickness. Since the new parameter set is applied with the first layer of the new layer thickness more energy than required for the actual powder layer thickness is used during the transition from 20 μm to 60 μm . When changing the layer thickness from 60 μm to 20 μm less energy than required for the given layer thickness is applied in the transition area.

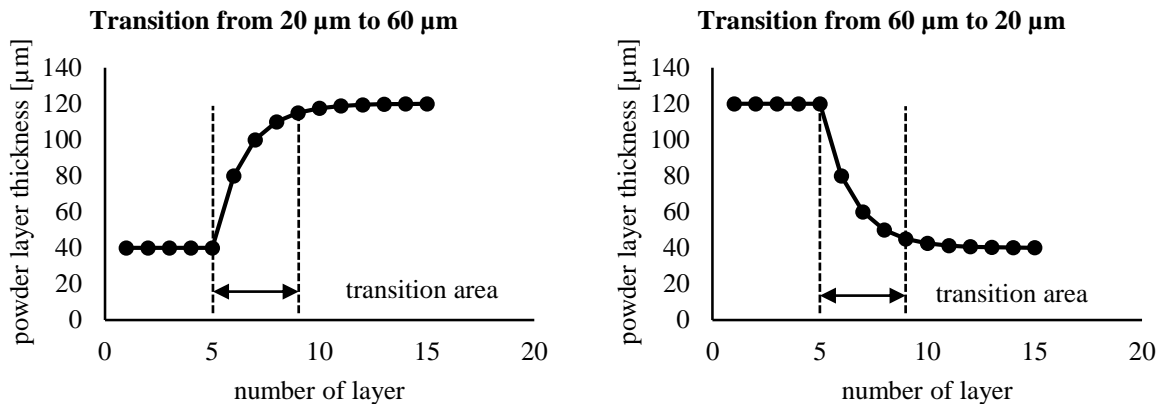


Figure 5: powder layer thickness at different layer thicknesses

The results of the mechanical testing and the micrographs indicate no defects or lack of fusion in the transition area for the specimens of case 3 and 4 where a lack of energy is present. The increased melt pool depth from the thicker powder layer is visible in figure 4. In the inclined specimens the lack of energy in the transition area results in large defects when transitioning from 60 μm to 20 μm . To prevent this an adjusted parameter set could be used in the transition zone or an increased overlap in the horizontal plane could be used to prevent lack of fusion.

6. Summary and outlook

The present work has the aim to increase build rates in the SLM process by dividing parts into different sections and building them using different layer thicknesses. The focus is set to the mechanical properties of these hybrid specimens and the interface section between the different layer thicknesses. From the results the following conclusions can be drawn:

- Using a layer thickness of 60 μm can increase the build rate from 2 mm^3/s up to 6.48 mm^3/s without reducing the mechanical strength of the material in the as built condition.
- Increasing the layer thickness increases the overall process efficiency.
- In the used test setup mechanical failure of hybrid tensile test specimens does not occur in the interface area but in the area of the weaker material.
- Adding a 20 μm section on top of a 60 μm section in inclined specimen results in large pores and leads to a decrease in ductility.

Combining different layer thicknesses in the SLM process is a feasible approach to increase build rates in part sections where no high accuracy and surface quality is required. The alignment of the interface area towards the build direction must be considered when designing those sections. Overlap strategies have to be developed for different interface angles and adjusted process parameters for the transition area. In future studies process parameters for different interface types will be investigated and a software to apply them to different geometries will be developed.

Acknowledgments

This work was partially funded by the Federal Ministry of Education and Research (BMBF Grant No. 02P15B035) and supported by Projektträger Karlsruhe (PTKA). The Authors would like to thank for this support.

References

- [1] ASTM F2792-12a (2012) Terminology for Additive Manufacturing Technologies, West Conshohocken, PA
- [2] Meiners W (1999) Direktes selektives Laser-Sintern einkomponentiger metallischer Werkstoffe. Shaker, Aachen
- [3] Kamath C, El-dasher B, Gallegos GF, King WE, Sisto A (2014) Density of additively-manufactured, 316L SS parts using laser powder-bed fusion at powers up to 400 W. Int J Adv Manuf Technol. doi:10.1007/s00170-014-5954-9

- [4] Gu DD, Meiners W, Wissenbach K, Poprawe R (2012) Laser additive manufacturing of metallic components: materials, processes and mechanisms. *International Materials Reviews* 57(3):133–164. doi:10.1179/1743280411Y.0000000014
- [5] Shi X, Ma S, Liu C, Chen C, Wu Q, Chen X, Lu J (2016) Performance of High Layer Thickness in Selective Laser Melting of Ti6Al4V. *Materials (Basel)* 9(12). doi:10.3390/ma9120975
- [6] Ma M, Wang Z, Gao M, Zeng X (2015) Layer thickness dependence of performance in high-power selective laser melting of 1Cr18Ni9Ti stainless steel. *Journal of Materials Processing Technology* 215:142–150. doi:10.1016/j.jmatprotec.2014.07.034
- [7] Delgado J, Ciurana J, Rodríguez CA (2012) Influence of process parameters on part quality and mechanical properties for DMLS and SLM with iron-based materials. *Int J Adv Manuf Technol* 60(5-8):601–610. doi:10.1007/s00170-011-3643-5
- [8] Boschetto A, Bottini L, Veniali F (2017) Roughness modeling of AlSi10Mg parts fabricated by selective laser melting. *Journal of Materials Processing Technology* 241:154–163. doi:10.1016/j.jmatprotec.2016.11.013
- [9] Greitemeier D, Dalle Donne C, Syassen F, Eufinger J, Melz T (2015) Effect of surface roughness on fatigue performance of additive manufactured Ti–6Al–4V. *Mater. Sci. Technol.*:1743284715. doi:10.1179/1743284715Y.0000000053
- [10] Stoffregen HA, Butterweck K, Abele E (2014) Fatigue Analysis in Selective Laser Melting: Review and Investigation of Thin-walled Actuator Housings. In: Bourell D (Hrsg) 25. Solid Freeform Fabrication Symposium, S 635–650
- [11] Schleifenbaum H, Diatlov A, Hinke C, Bültmann J, Voswinckel H (2011) Direct photonic production. Towards high speed additive manufacturing of individualized goods. *Prod. Eng. Res. Devel.* 5(4):359–371. doi:10.1007/s11740-011-0331-0
- [12] EOS GmbH Electro Optical Systems (2018) EOS System Data Sheet EOS M 290. https://www.eos.info/systems_loesungen/download/system_datenblatt_M-290.pdf
- [13] Spierings AB, Schneider M, Eggenberger R (2011) Comparison of density measurement techniques for additive manufactured metallic parts. *Rapid Prototyping Journal* 17(5):380–386. doi:10.1108/13552541111156504
- [14] Deutsches Institut für Normung e.V. (2009) Prüfung metallischer Werkstoffe – Zugproben (50125:2009-07)
- [15] EOS GmbH Electro Optical Systems (2014) Material Datasheet - EOS StainlessSteel 316L. EOSINT M290 400W System mit EOSPRINT 1.0 und Parametersatz 316L_Surface 1.0
- [16] Petzow G (1999) Metallographic etching. Techniques for metallography, ceramography, plastography, 2. Aufl. ASM International, Materials Park, OH

- [17] Buchbinder D, Schleifenbaum H, Heidrich S, Meiners W, Bültmann J (2011) High Power Selective Laser Melting (HP SLM) of Aluminum Parts. *Physics Procedia* 12:271–278. doi:10.1016/j.phpro.2011.03.035